2002

Wintertime Shoreward Near-Surface Currents South of Cape Hatteras

Dana K. Savidge
Old Dominion University

Original Publication Citation

Savidge, D. K. (2002). Wintertime shoreward near-surface currents south of Cape Hatteras. *Journal of Geophysical Research: Oceans, 107*(C11), 3205. doi:10.1029/2001jc001193

Wintertime shoreward near-surface currents south of Cape Hatteras

Dana K. Savidge

Center for Coastal Physical Oceanography, Department of Ocean, Earth and Atmospheric Sciences, Old Dominion University, Norfolk, Virginia, USA

Received 30 October 2001; revised 16 May 2002; accepted 22 May 2002; published 27 November 2002.

[1] Cross-isobath flow on continental shelves is of interest for a variety of reasons. Near Cape Hatteras, North Carolina, the transport of larval organisms, pollutants, and oceanic carbon budget constituents to and from the adjacent Albemarle and Pamlico Sounds may depend critically on cross-isobath currents. Shoreward currents in the near-surface waters south of Cape Hatteras are documented herein, on the basis of continuous 2-year time series, encompassing all or part of three consecutive winters. Energetic shoreward currents exist ~30% of the time from midfall through late spring. These currents are evident over the 20 and 35 m isobaths along a mooring line situated ~40 km southwestward from Cape Hatteras. Shoreward velocities average ~12 cm/s, and events persist from 0.5 to 4 days, occurring every 2.5–5 days, except in summer. These events often coincide with southwestward winds but occur under both upwelling and downwelling favorable conditions, such that Ekman veering in the surface layer does not account for the shoreward velocities. In winter the mooring line south of Cape Hatteras is frequently traversed by a strong temperature and salinity front, with light, relatively fresh, cold, stratified water on one side, and denser, more saline, warmer, unstratified water on the other. Hydrography and satellite sea surface temperature imagery help identify this front as the boundary between South Atlantic Bight and Mid-Atlantic Bight coastal shelf waters, the ''Hatteras Front.'' Flow along the Hatteras Front where it crosses the shelf appears to account for the observed shoreward currents. The along-shelf advection of the Hatteras Front may depend on both winds and Gulf Stream distance offshore. *INDEX TERMS:* 4219 Oceanography: General: Continental shelf processes; 4223 Oceanography: General: Descriptive and regional oceanography; 4227 Oceanography: General: Diurnal, seasonal, and annual cycles; 4528 Oceanography: Physical: Fronts and jets; *KEYWORDS:* mesoscale fronts, cross-shelf transport, Cape Hatteras

Citation: Savidge, D. K., Wintertime shoreward near-surface currents south of Cape Hatteras, *J. Geophys. Res.*, *107*(C11), 3205, doi:10.1029/2001JC001193, 2002.

1. Introduction and Background

[2] Cross-isobath flow on the continental shelf has long been of interest for a variety of reasons. Near Cape Hatteras, North Carolina, the transport of the larvae of commercially important organisms, pollutants, and constituents of the oceanic carbon budget to and from the adjacent Albemarle and Pamlico Sounds may depend critically on such flow. In the past, investigators have advanced a number of mechanisms that might account for shoreward transport south of Cape Hatteras. Ekman drift associated with the predominantly southwestward winter winds [*Nelson et al.*, 1977], upwelling at the Gulf Stream shoreward edge resulting in a shoreward buoyancy current [*Checkley et al.*, 1988], advection by shoreward moving Gulf Stream filaments [*Stegmann and Yoder*, 1996], advection by the southward extension of cold fresh Mid-Atlantic Bight (MAB) shelf water past Cape Hatteras into the South Atlantic Bight (SAB) [*Stegmann and Yoder*, 1996], and internal waves [*Shanks*, 1988] have all been discussed as plausible mechanisms. *Quinlan et al.* [1999] suggest that menhaden eggs and larvae may rely on a combination of along-shelf transport from northern spawning grounds and a retentive wind-driven gyre circulation in Raleigh Bay during winter to advect the eggs and larvae into the nearshore regime. Species whose life histories do not include the large seasonal along-shelf migration seen in the menhaden life cycle may rely more directly on effective mechanisms for short-term rapid shoreward advection. Further, the short reproductive lifespans of some species suggest that whatever the most effective mechanism is, it should be a robust and reliable one, since the failure of consecutive year classes could doom such populations (C. Jones, personal communication, 2001).

[3] In this paper, shoreward currents in the surface waters (5 m depth) of Raleigh Bay are documented on the basis of continuous 2-year time series of currents measured with moored instrumentation. Shoreward currents are evident

0148-0227/02/2001JC001193

approximately 29% of the time in the winter (October–March), under both downwelling favorable and upwelling favorable wind conditions. These shoreward currents are evident at the 20 and 35 m isobaths along a mooring line situated ~40 km southwestward from Cape Hatteras, and also appear approximately 10% of the time at the 60 m isobath (the shelf break). Both wind field variability in winter and Gulf Stream variability are implicated, but in both cases, the effect seems to be indirect. The primary cause appears to be along-front advection along an along-shelf translating cross-shelf density front. This front separates warmer, saltier SAB water from cold fresh MAB water. The effects the Gulf Stream and the winds have on advecting this front along-shelf appears to account for their bearing on cross-shelf transport.

[4] The front itself, termed the "Hatteras Front" by *Churchill and Berger* [1998], is defined by a density contrast of several σ_t units, the result of strong temperature and salinity gradients along-shelf that do not completely compensate each other. The contrast in temperature and salinity properties between the coastal water masses south and north of Cape Hatteras have been described by *Bumpus* [1973] and *Pietrafesa et al.* [1994]. It is well established that the source regions for shelf water in the southern MAB and the northern SAB are distinctly different. The relatively cooler fresher water that converges on Cape Hatteras from the north is influenced both locally, by the cold fresh outflow from the Chesapeake and Delaware Bays in the winter, and remotely, from the northern MAB and beyond, as the mean southward flow along the MAB conveys water southward [*Stefansson et al.*, 1971; *Bumpus*, 1973; *Chapman and Beardsley*, 1989; *Berger et al.*, 1995]. The generally northward drifting coastal water of the SAB consists of warm, southern origin water that has been "salted" along its path by its close proximity to the Gulf Stream, through both stranded Gulf Stream filaments and upwelled deep Gulf Stream water, with relatively little riverine freshwater influx [*Stefansson et al.*, 1971; *Bumpus*, 1973; *Atkinson*, 1977].

[5] The idea that the intrusion of MAB water past Cape Hatteras into the SAB can affect the circulation on the shelf south of Cape Hatteras is not new. *Stefansson et al.* [1971], using data from a series of hydrographic surveys and drifter releases, center their discussion of circulation on the North Carolina shelf on the dynamic topography of MAB shelf water intrusions into Raleigh Bay and beyond. They document shoreward currents near the surface in Onslow Bay of approximately 9 cm s^{-1} magnitude. *Bumpus* [1973] recounts observations of advection of the front southward past Cape Hatteras. *Stegmann and Yoder* [1996] have shown the front progressing southward past Cape Hatteras into Raleigh Bay and beyond in satellite Advanced Very High Resolution Radiometer sea surface temperature (AVHRR SST) imagery, and have suggested that the front may play a role in the shoreward advection of larvae in winter south of Cape Hatteras, though they do not specify the particular mechanism whereby such transport could occur. The displacement of the Hatteras Front southward past Cape Hatteras has been explored by *Pietrafesa et al.* [1994], who found high correlation between the salinity at Diamond Shoals (the shallow shelf area extending offshore from Cape Hatteras) and the along-shelf wind component, concluding that the front separating MAB and SAB water was advected in the along-shelf direction by fluctuating winds. The Hatteras Front affects circulation north of Cape Hatteras as well. *Churchill and Berger* [1998] investigated the approximately alongshore oriented portion of the Hatteras Front, and examined its role in the export of MAB water from the shelf to the slope and beyond. This may account for the relationship [*Savidge and Bane*, 2001] see between Gulf Stream position and along-shelf convergence and offshore export immediately north of Cape Hatteras, through Gulf Stream effects on the Hatteras Front.

2. Data

[6] The data used in this study were collected by a multi-institutional team funded by the Minerals Management Service [*Berger et al.*, 1995]. Fifteen mooring locations across and along the Cape Hatteras shelf and slope were maintained from March 1992 through February 1994 (Figures 1 and 2). These moorings were situated along three cross-shelf lines bracketing Cape Hatteras, and one along-shelf line at the shelf edge. Preliminary findings were summarized in a technical report at the conclusion of the field project [*Berger et al.*, 1995].

2.1. Current Meter Observations

[7] Currents on the shelf were measured with InterOcean S4 and General Oceanic MkII winged current meters, with S4s at 5 m and 14.3 m at the 20 m isobath stations, and also at 5 m depth on the 35 and 60 m isobath stations. In the following, moorings are named according to the line they are on, and their position offshore on the line. For example, the 20 m isobath mooring on the B line is mooring B1, and the 35 m isobath mooring on the C line is mooring C2. Instrument packages are numbered increasing downward, so that the 5 m depth package at C2 is referred to as $C2_1$, while the 20 m depth package is $C2_2$. The data have been filtered and subsampled as follows. Raw data were 3-hour low-pass (3-HLP) filtered with a Lanczos kernal and subsampled to hourly values. These hourly data were then processed with a 48-HLP Hanning filter and subsampled to daily noon values, or with a 24-HLP Hanning filter and subsampled to 6-hourly values on the quarter day. The daily data are used to illustrate the seasonal nature of the shoreward currents, and the wind, shelfwide current, temperature and salinity evolution associated with them. The 6-hourly data are used to calculate summary statistics and to illustrate the evolution of particular shoreward flow events.

[8] In the following, shoreward oriented currents at moorings C1 and C2 are demonstrated and analyzed. The definition of the shoreward direction is characteristically problematic when discussing cross-isobath motion, so that some discussion of the definition used here is warranted. Instead of attempting the difficult and error prone resolution of measured currents into along-shelf and cross-shelf components, a more flexible approach has been taken. A range of directions have been identified which are shoreward of alongshore at the C2 mooring location, and appear to be clearly across the general trend of bathymetry toward shallower depths at that location. Angles from 85° to 185° counterclockwise (CCW) from due east have been chosen

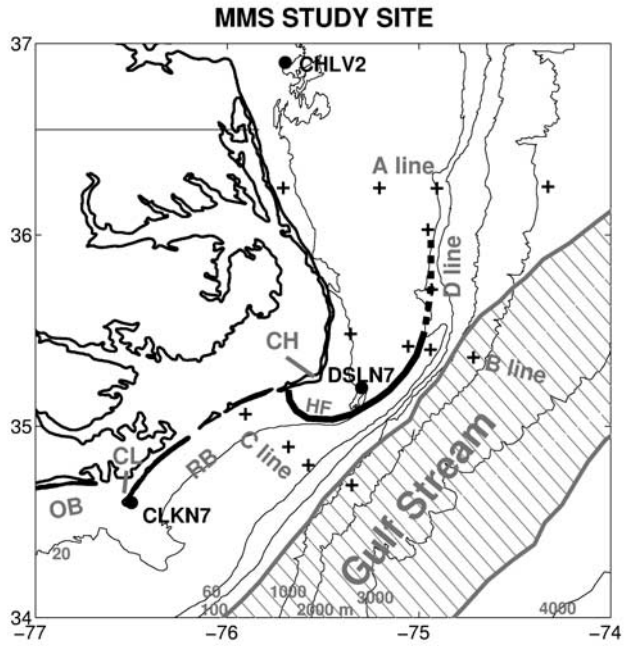

Figure 1. Cape Hatteras continental shelf/slope field study site (March 1992 to February 1994). Mooring locations (pluses) along three cross-shelf lines (lines A, B, and C) and one shelf edge line (line D) and C-MAN meteorological stations (solid circles) are shown. A schematic Hatteras Front, labeled ''HF'' and a schematic Gulf Stream are shown. The northward extent of the Hatteras Front and the extent to which it is contiguous with the Gulf Stream front southeast of Cape Hatteras are unknown. Cape Hatteras (CH), Cape Lookout (CL), Raleigh Bay (RB), and Onslow Bay (OB) are labeled.

as suitable for this definition. The clockwise (CW) limit (85°) was set by the eastward extent of the North Carolina coastline in Raleigh Bay. Flow at mooring C2 oriented CW from that limit would miss the coast if it travelled in a straight line from the mooring along the radius. The CCW limit (185°) was chosen as the angle approximately parallel with the trend of the 20 m isobath north of mooring C2. This choice was guided by the notion that the direction of along-shelf flow at C2 might depend either on the local orientation of the bathymetry (the 35 m isobath in Raleigh Bay runs essentially parallel to the shelf edge, represented in many of these plots as the 60 m isobath) or on the orientation of the coastline and bathymetry against which an offshore sloping sea surface gradient might develop. Although flow oriented between 185° and approximately 210° CCW of east is directed landward from C2 in Raleigh Bay, it is not clear that this flow is not simply oriented alongshore relative to the shoreline or shallower bathymetry somewhere to the north-northwest of the mooring. The 185° threshold seems reasonable on a second basis as well: histograms of surface current direction at $C2_1$ show a large quantity of days with currents oriented in the 190–210° bins, which are turned just CW of the predominant current directions at the 20 m depth, which are presumably alongshore (the principal axis for the $C2_2$ current record is oriented 26° CCW of east). The 185° threshold effectively eliminates this subset of currents at 5 m depth which are (1) oriented just to the right of the alongshore direction preferred in the mid-water column, so (2) could easily be argued to represent Ekman turning. In other words, this threshold selects against the common current direction at $C2_1$, which is likely to be oriented slightly to the right of alongshore due to Ekman drift. Shoreward currents at moorings C1 and C3 are defined using the same criterion used at mooring C2. When shoreward currents are discussed at mooring B1, a similar definition is utilized, defined as the quadrant between 135 and 225° CCW of east.

2.2. Temperature and Salinity

[9] Temperature and salinity (and pressure at the slope moorings) were measured by the current meters deployed, and were filtered as described above. However, for the mooring C2 salinity record presented here, an additional adjustment was made after the low-pass filters were applied. Salinity records require calibration at frequent intervals to assure that sensor drift and constant offsets are accounted for. Unfortunately, the hydrographic data in this experiment are not dense enough in space or time to adequately

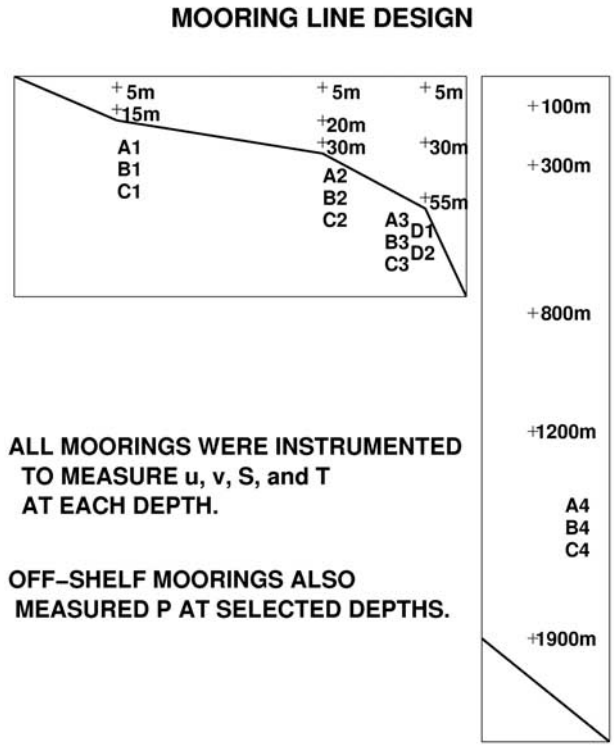

Figure 2. Schematic mooring line design. Shelf moorings were situated at the 20, 35, and 60 m isobaths, with slope moorings at the 2000 m isobath. Mooring numbers increment from 1 to 4 in the seaward direction. (left) Shelf and shelf edge moorings had two to three instrument packages in the vertical, including InterOcean S4 and General Oceanic MkII winged current meters (u, v), with temperature (T) and salinity (S) sensors. (right) Deeper moorings had five to six instrument packages in the vertical, including General Oceanic MkI/MkII winged current meters and Aanderaa RCM 7/8s, with T, S, and pressure (P) sensors.

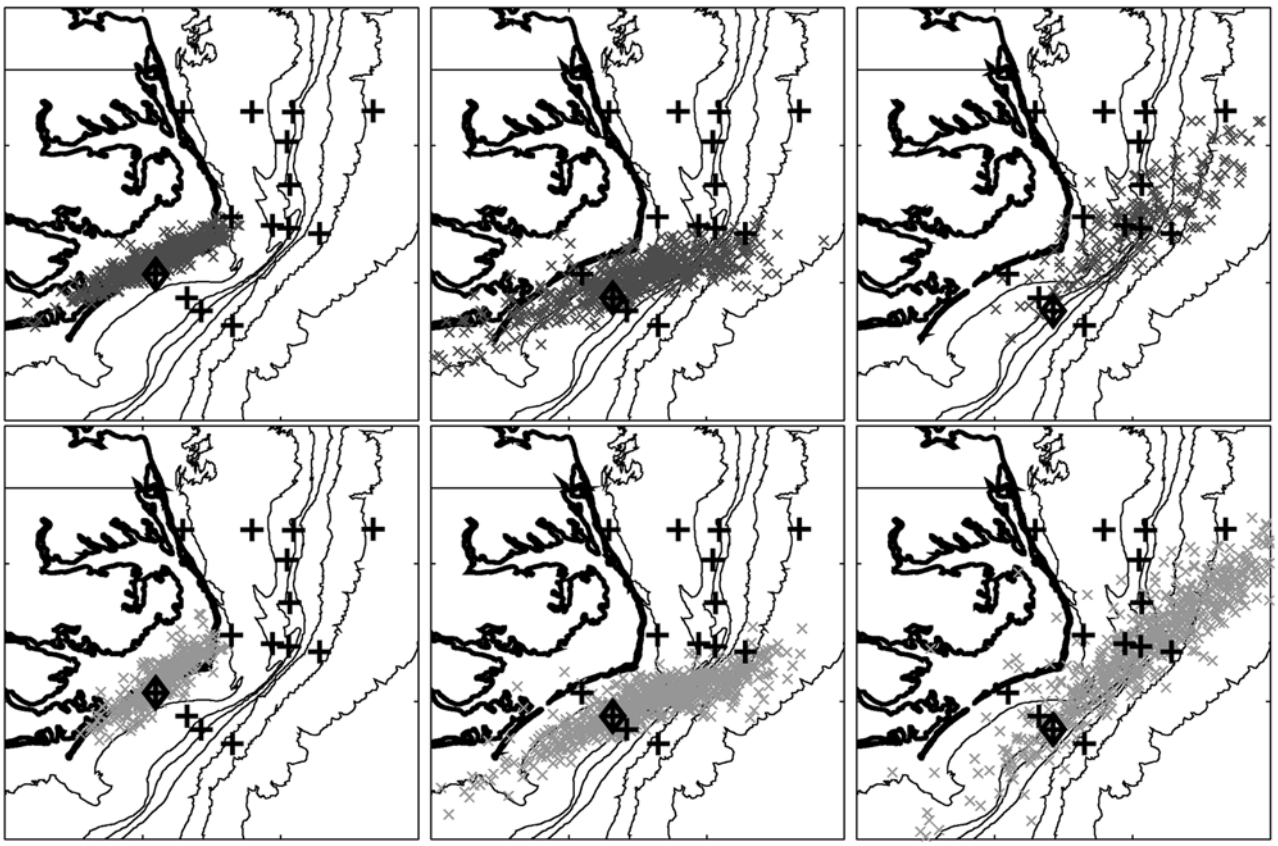

Figure 3. Three-day PVD endpoints for velocity data from the C mooring line. The origin is shown as a bold diamond with a cross. Data are calculated from (top) the 5 m depth current meter records and (bottom) the second instument level down on each mooring for (left) mooring C1, (middle) mooring C2, and (right) mooring C3. The 20, 40, 60, 100, 1000, 2000, and 3000 m isobaths are shown.

accomplish this. The short-term variability of the salinity over hours and days discussed in the following sections is expected to be well represented in magnitude without correction. However, the completely uncorrected salinity records imply that the lower water column was unstable for significant fractions of the experiment time. Since this is obviously nonphysical, a simple correction technique was applied to remove some of the low-frequency offsets from the 20 and 30 m depth records, relative to the 5 m depth values, which should be correct to within 0.5 psu (P. Hamilton, personal communication, 2001). Briefly, the 24-HLP temperature time series were examined to find instances of small vertical temperature gradients (less than 0.075°C difference), indicating well-mixed conditions. Assuming well-mixed salinity on those dates, offsets between the measured salinities at 20 and 30 m and the 5 m depth salinities were calculated. These sporadic corrections were then interpolated to 6-hourly values, smoothed over 15 days, and used to adjust the 48-HLP and 24-HLP salinity records at 20 and 30 m depth. This method does not work well for the summer periods of the data, when no well-mixed episodes were indicated by the temperature records, or when no 5 m level temperature or salinity records exist.

2.3. Winds

[10] Hourly wind data from three National Data Buoy Center Coastal Marine Automated Network (C-MAN) Stations located near Cape Hatteras were used in this study (Figure 1): CHLV2, near Cape Henry on the southern side of Cheasapeake Bay; DSLN7, off Cape Hatteras over Diamond Shoals; and CLKN7, off Cape Lookout. These data were then processed with a 48-HLP Hanning filter and subsampled to daily noon values, or with a 12-HLP Hanning filter and subsampled to 6-hourly values on the quarter day. While the ocean data were 24-HLP to remove the large tidal signal, the wind data shows a far less energetic tidal signal, so that 12-HLP filtering is sufficient, thus assuring that as much information about the turning of the wind is preserved as possible in the 6-hourly subsampled filtered data. Short gaps in the DSLN7 data were filled with CLKN7 winds, with means and standard deviations adjusted to match those at DSLN7.

2.4. Gulf Stream Position

[11] As discussed by *Savidge and Bane* [2001], moorings B4 and C4 were imbedded in the Gulf Stream's cyclonic flank throughout most of the experiment. Of the variables measured by the uppermost instrument packages there, pressure proves to be most useful as an indicator of Gulf Stream position. Since the mooring is not rigid, the mooring line is pulled down in the water column by the integrated effect of the large Gulf Stream currents [*Hogg*, 1991] as the Gulf Stream jet shifts toward the shelf edge. The pressure records indicate how far in the vertical the particular

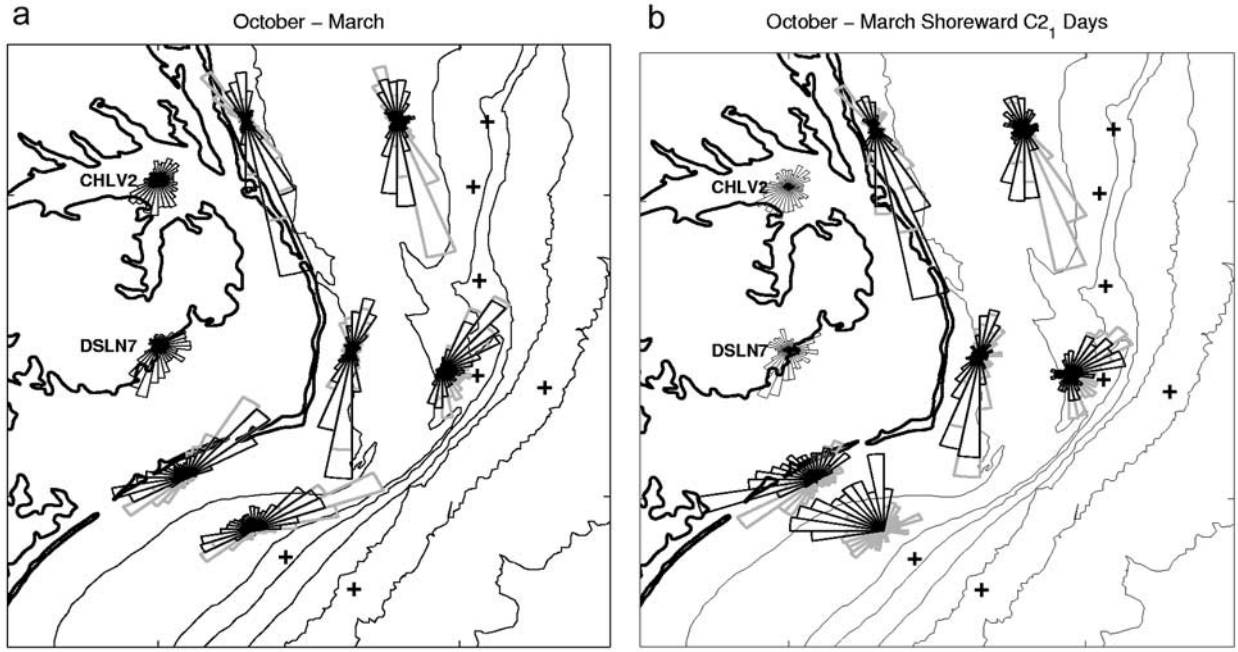

Figure 4. Polar histograms for wind and current direction at the 20 and 35 m isobath mooring locations (6-hourly data): (a) data from October–March and (b) data from October–March when currents at $C2_1$ were shoreward. The 5 m depth data are solid; the second level down are shaded. The ocean current direction histograms are plotted with their origins on the mooring locations. The wind direction polar histograms for CHLV2 and DSLN7 (as labeled) are plotted to the west of the current meter mooring array, not at the locations where the data were taken. The current angles were calculated fr'om the 24-HLP current meter data and were sorted into 10° bins centered at 5, 15, . . ., 355° CCW from east. Totals in each bin have been normalized by sample size. The histograms are plotted so that the length of the pie slice oriented in a particular direction represents the number of data points when flow fell within that pie slice.

mooring has been dragged down, and varies monotonically with the integrated current velocity impinging on the mooring line. Visual comparison and cross-spectral analysis between the pressure records at the upper instrument packages at moorings B4 and C4 and the velocity records at 100, 1200, and 1900 m depth at moorings B4 and C4 indicate that the large surface intensified Gulf Stream velocities dominate the pressure records. The pressure fluctuations are strongly correlated with episodes of strong northeastward flow in the upper current meter records, and not with strong southwestward filament pulses in the upper water column or with lower water column fluctuations [*Savidge and Bane*, 2001].

3. Observed Cross-Shelf Currents

[12] The primary result to be reported in this paper is the direct measurement of shoreward currents in the upper water column on the midshelf immediately south of Cape Hatteras. Their existence is evident in progressive vector diagrams (PVDs) constructed for all three day periods in the data, (Figure 3, where PVD endpoints are plotted, relative to their origins, the mooring locations).

[13] Despite predominantly along-shelf distribution of the PVD endpoints, shoreward currents are evident at 5 and 14.3 m depths at C1, at the 5 and 20 m depths at C2, and occasionally at the 5 and 30 m depths at C3. This is also true if longer periods are used to construct PVDs, up to 10 days or so. The shoreward tendency in the PVDs is of sufficient magnitude to advect parcels of water quite close to the shore over very short time periods, if similar flow extended all the way to the shore. Naturally it is understood that PVDs do not represent true parcel trajectories, since they are constructed from velocity data only at the mooring locations. It is unfortunate that the bottom mooring records along the C line, $C2_3$ and $C3_3$ showed evidence of complex compass errors over much of the deployment, such that bottom cross-shelf currents cannot be investigated on the C-line with this data set.

[14] Polar histograms of current direction also illustrate the existence of shoreward or seaward currents (Figure 4). Shelf currents were primarily oriented alongshore at all locations. Note that for moorings A1, A2, and B2, the most predominant current directions at 5 m depth are oriented 0–30° CW from the predominantly alongshore current directions at 20 m depth, consistent with Ekman veering in the surface layer. The A1 and B1 moorings suggest smaller surface rotations than the A2 mooring, consistent with the smaller rotation expected at the surface in a shallower coastal environment [*Madsen*, 1977]. At moorings C1 and C2, the most predominant current directions at 5 and 20 m depth are oriented along-shelf. However, off the along-shelf

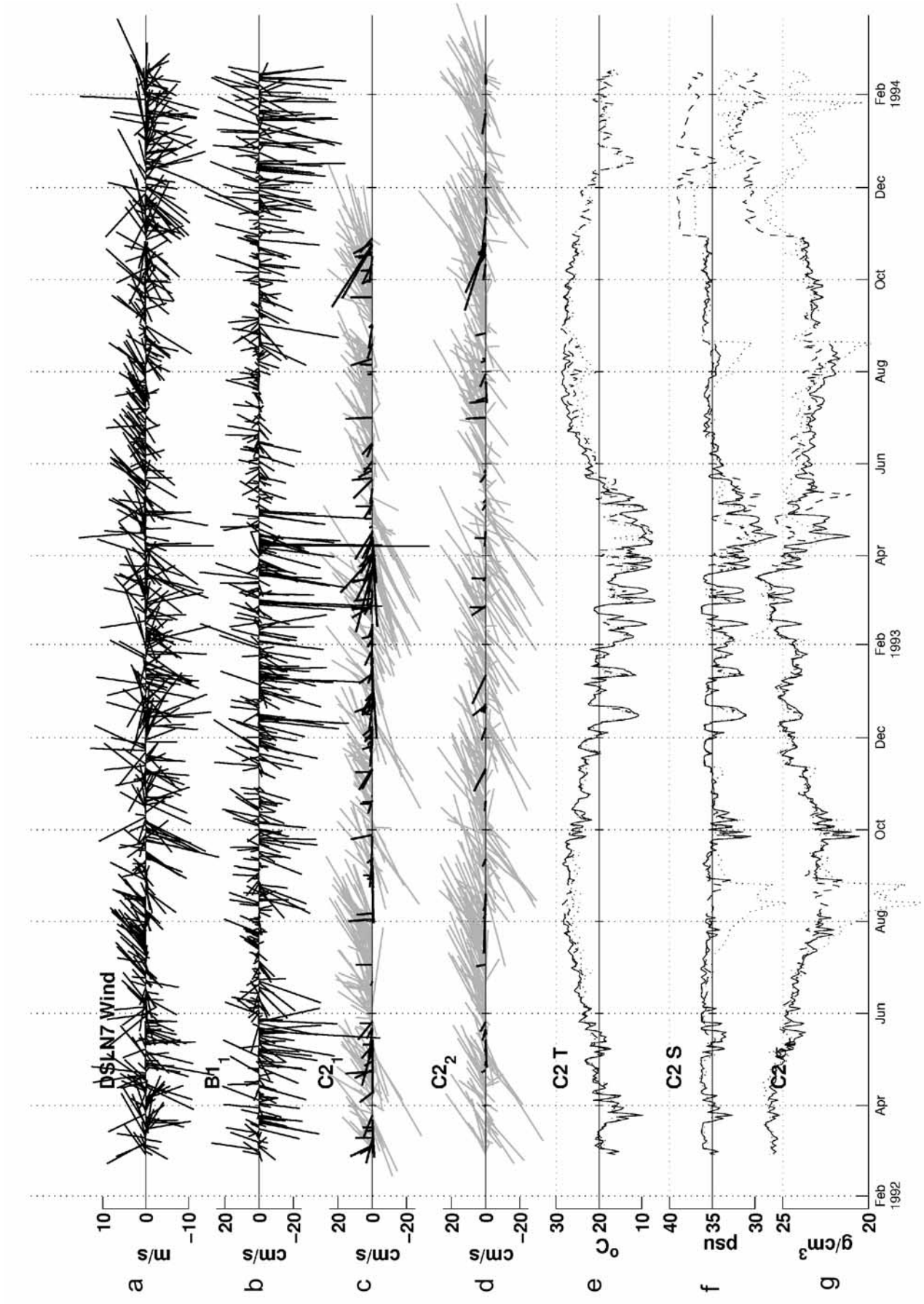
a
m/s
10
0
−10
DSLN7 Wind
b
cm/s
20
0
−20
B1 1
c
cm/s
20
0
−20
C2 1
d
cm/s
20
0
−20
C2 2
e
°C
30
20
10
C2 T
f
psu
40
35
30
C2 S
g
g/cm³
25
20
C2 6
Feb 1992
Apr
Jun
Aug
Oct
Dec
Feb 1993
Apr
Jun
Aug
Oct
Dec
Feb 1994

principle axis, shoreward currents predominated over seaward currents at $C1_1$, $C1_2$, $C2_1$, and $C2_2$. Days of shoreward currents at $C2_1$ (Figure 4b) were characterized by predominantly southwestward (downwelling favorable) winds and southward or southwestward along-shelf currents at moorings A1, A2, B1, B2, and at middepth at C2.

[15] However, shoreward currents at $C2_1$ occur under conditions of upwelling favorable winds as well, concurrent with shelf currents oriented to the north or northeast at moorings A1, A2, B1, B2, and at middepth at C2. Note that for northeastward currents at 20 m depth at C2, the most predominant current directions at 5 m depth are not oriented 0–30° CW from the most predominant current directions at 20 m depth, as they would be if Ekman veering dominated during the shoreward events at C2.

[16] It is reassuring that the net shoreward displacements calculated from the 48-HLP data appear in four separate time series, representing data from two different types of current meters. Further, no shoreward preference appears in the high-passed data from the same mooring records, with many instances of flow in the seaward directions evident in the polar histograms of directions of the high-passed currents (not shown).

[17] The long-term variability of some relevant time series over the period of the experiment (Figure 5) is instructive. Looking first at the DSLN7 wind record, note that during late June, July, and August of both years, winds are primarily northeastward, with very few instances of wind to the southwest. During summer, along-shelf currents at mooring $B1_1$ were predominantly northward and of relatively low magnitude. During August, September, and October, the wind became more variable and more energetic, with the mean shifting from northeastward to southwestward. Currents at $B1_1$ also became more energetic to the south. By sometime in November, the winds shifted to a wintertime regime, with highly variable but predominantly southwestward strong winds. These strong winds dominate the winter variability, and persist through April. They are accompanied by strong, highly variable along-shelf currents at $B1_1$ (and $B1_2$, not shown) that are highly correlated with the wind, and southward in the mean. These too taper off by late April, with occasional bursts through May of both years.

[18] Currents at C2, 5 and 20 m depths, are primarily along-shelf (approximately 26° CCW of eastward). Variability is highly correlated with along-shelf wind at DSLN7, with along-shelf currents at $B1_1$, and with depth (Figure 5). During summer, the currents are predominantly northeastward, shifting to highly variable flow with strong southwestward events during fall through winter. Conspicuous at the 5 m depth record are bursts of shoreward currents. Flow oriented between 85° and 185° CCW of east has been plotted in black, in contrast to the remainder of the vectors plotted in grey, to emphasize these shoreward events. These events are most common in December through March, but commence in fall and persist through April and into May. They appear to peak during or immediately following the times of most southward wind and the largest southward pulses of flow at B1. They are almost absent in June and July, with shoreward events appearing to ramp up in magnitude and incidence in August through October. Occasionally the middepth currents at C2 also turn shoreward.

[19] Temperature records at C2 show a seasonal cycle at all depths, as do the density records. The general cooling from late August and September through March is punctuated by large abrupt changes in temperature at all levels, often exceeding a 5°C change in less than 2 days. These temperature changes are accompanied by sharp salinity changes of several psu, also occurring at all levels, and highly correlated with the temperature variability. Apparently a temperature and salinity front traverses the vicinity of mooring C2 throughout the winter months. This front has cold, fresh, often vertically stratified water on one side, and warmer, saltier, unstratified water on the other. The salinity and temperature do not completely compensate each other, such that the cold fresh water is less dense than the warm salty water, as seen in the density time series for all levels. Note that the expected signature of Gulf Stream filaments crossing the mooring location would be quite different: cool unstratified winter shelf water would be replaced by warmer, saltier, more stratified water, with the warm salty water mass being the lighter component (hence the surface expression of filaments on the shelf in AVHRR SST data).

[20] The shoreward currents are not limited to the midshelf, but are also seen over the 20 m isobath (C1) and occasionally over 60 m isobath at the shelf edge (C3) (Figure 6). There are frequent large changes in T over short timescales at C1 in winter. At C3, the shoreward currents are much more sporadic, but can be quite energetic at times (note the change in axis limits in the C3 stickplots). At B1, particularly in 1993, large temperature excursions and a higher incidence of shoreward currents occurs in summer rather than in winter.

4. Shoreward Current Event Characterization

[21] A summary description of the shoreward currents follows, with an emphasis on data from October–March. These months, referred to in the following as 'winter', were chosen based on the seasonal progression of winds, temperature variability, and shoreward current events, as described relative to Figure 5. From October through March, there were shoreward currents 29% of the time at $C2_1$ in the 24-HLP data. (For comparison, currents were shoreward at 5 m depth at A1, A2, B1, or B2 less than 8% of the time in winter.) The distribution of shoreward daily velocity angles

Figure 5. (opposite) The 48-HLP ronald time series: (a) DSLN7 wind, (b) $B1_1$ currents, (c) $C2_1$ currents, (d) $C2_2$ currents, (e) C2 temperature (all depths), (f) C2 salinity (all depths, corrected), and (g) C2 density (all depths). North is aligned with the positive y axis in the stick plots. In Figures 5c and 5d, solid vectors represent currents oriented between 85° and 185° CCW of eastward, while the shaded vectors represent all other current orientations. In Figures 5e–5g, solid lines represent data from 5 m depth, dashed lines represent data from 20 m depth, and dotted lines represent data from 30 m depth. Note the end of summer periods when 5 m densities appear to exceed densities deeper in the water column. These were periods when the salinity records showed substantial drift problems, but no well-mixed water column episodes existed to estimate adjustments of the 20 and 30 m salinities.

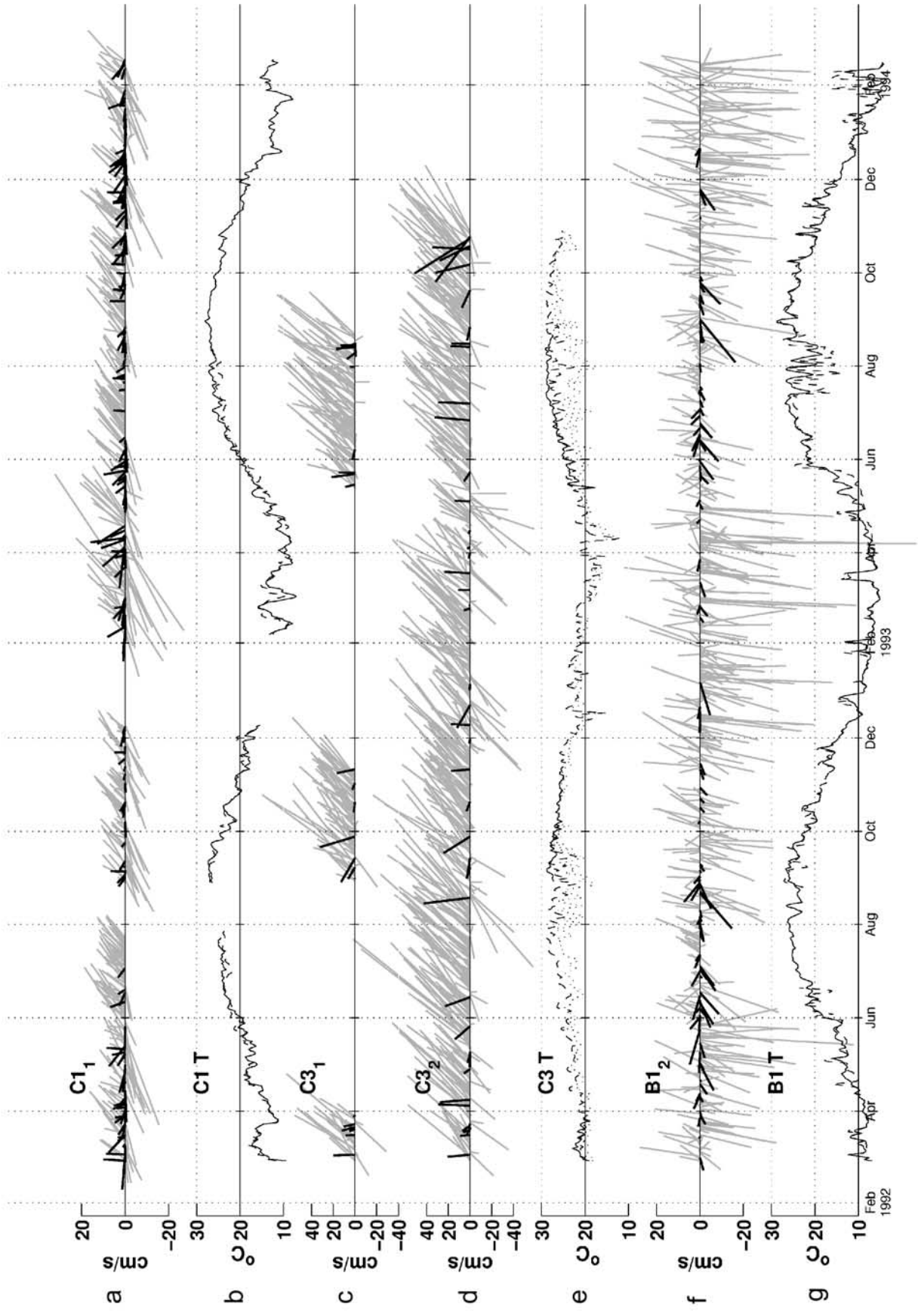
a
b
c
d
e
f
g
C1 1
C1 T
C3 1
C3 2
C3 T
B1 2
B1 T
cm/s
°C
Feb 1992
Apr
Jun
Aug
Oct
Dec
Feb 1993
Apr
Jun
Aug
Oct
Dec
Feb 1994

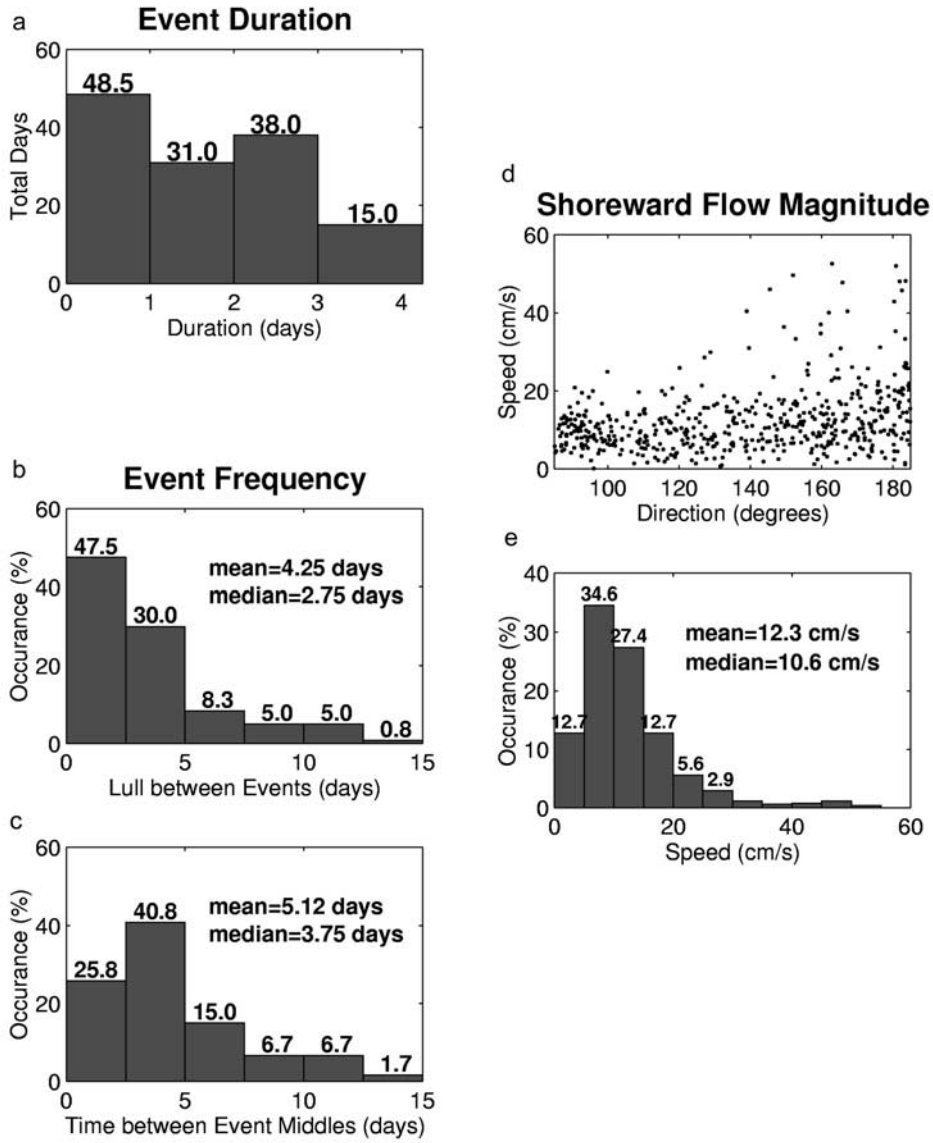

Figure 7. Characterization of shoreward flow events at mooring $C2_1$, using 24-HLP data: (a) histogram of event durations in total days, (b) histogram of length of lulls between the last data point of a shoreward event and the first data point of the next event, normalized by total event lulls and converted to percentages, (c) histogram of length between midpoints of two consecutive shoreward events, normalized by total event pairs and converted to percentages, (d) scatterplot of shoreward velocity magnitude as a function of current orientation (degrees CCW from east), and (e) histogram of shoreward velocity magnitude, normalized by total number of data points and converted to percentages.

at $C2_1$ illustrates broad coverage of the shoreward sector (Figure 4b). Winter currents at $C1_1$ were shoreward 29% of the time, and at $C3_1$ 14% of the time (out of a relatively gappy data set). October–March shoreward flow days at $C2_1$ were coincident with shoreward flow at $C1_1$ 49% of the time, and coincident with shoreward flow at $C3_1$ 18% of the time.

[22] The duration of shoreward events at $C2_1$ was estimated from 24-HLP data (Figure 7a). Periods of shoreward

Figure 6. (opposite) The 48-HLP time series: (a) $C1_1$ currents, (b) C1 temperature (both depths), (c) $C3_1$ currents, (d) $C3_2$ currents, (e) C3 temperature (all depths), (f) $B1_1$ currents, and (g) B1 temperature (both depths). North is aligned with the positive y axis in the stick plots. For the C line current meter data, solid vectors represent currents oriented between 85° and 185° CCW of eastward, while the shaded vectors represent all other current orientations. For the B1 current meter data, solid vectors represent currents oriented between 135° and 225° CCW of eastward, while the shaded vectors represent all other current orientations. In Figures 6b, 6e, and 6g, solid lines represent data from 5 m depth, dashed lines represent data from 14.3 (on the 20 m isobath) or 30 m depth (on the 60 m isobath), and dotted lines represent data from 55 m depth.

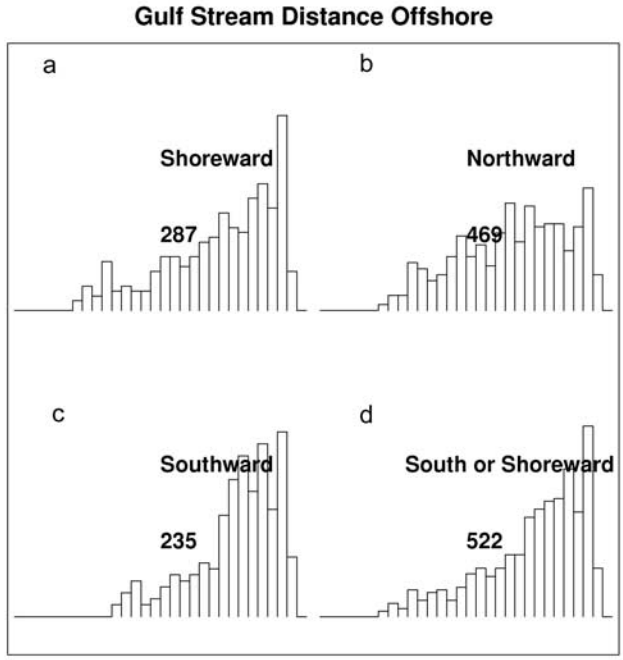

Figure 8. Histograms (from 24-HLP data) of Gulf Stream relative distance offshore along the B mooring line from October to March: (a) data when currents at $C2_1$ were shoreward, (b) data when currents at $C2_1$ were northward but not shoreward, (c) data when currents at $C2_1$ were southward but not shoreward, and (d) data when currents at $C2_1$ were southward or shoreward. The Gulf Stream proxies values show relative distance offshore, not absolute, so the histogram bin limits are not given. Bins representing a more shoreward Gulf Stream location are situated at the left of these histograms, while bins representing a more seaward Gulf Stream location are situated at the right. Histogram values have been normalized by the total number of data points used in each histogram, which are shown above each histogram.

flow interrupted by no more than one data point oriented not shoreward were considered continuous. (Only 12 single data point interruptions were found amongst the 518 total shoreward data points.) Most events lasted two days or less (79.5 cumulative days). However, a sum of 53 days of shoreward current occurred during shoreward events lasting 3–4 days. The maximum event duration was 4.25 days. During the shoreward events shoreward current speed averaged 12.3 cm/s, with slightly faster velocities at the CCW limit (Figures 7d and 7e). The frequency of shoreward events was characterized both by the time between events and the times between event midpoints (Figures 7b and 7c). 47.5% of the events were separated by 2.5 days of alongshore flow or less, with a total of 77.5% of the events separated by less than 5 days of alongshore flow. Times between event midpoints support a similar story, with 66.6% of the event midpoints separated by less than 5 days.

[23] Given the importance that previous authors have attached to the Gulf Stream concerning cross-shelf transport (see the references in section 1), histograms of the Gulf Stream distance offshore were constructed for the following bins (24-HLP data): winter days (October–March) when the currents at $C2_1$ were shoreward, winter days when the currents at $C2_1$ were northward but not shoreward, winter days when the currents at $C2_1$ were southward but not shoreward, and winter days when the currents at $C2_1$ were southward or shoreward. Comparing the histograms between the periods (Figure 8) shows that shoreward or southward days coincided with days that the Gulf Stream was relatively far from shore. Northward but not shoreward days coincided with days when the Gulf Stream was relatively close to shore.

5. Hatteras Front

[24] Several hydrographic cruises were conducted during the course of the experiment which effectively identify the front that crosses the C2 mooring location so frequently during the winter months. For example, data from two separate cruises in November of 1992 and August of 1993 are shown here, illustrating the horizontal structure of the 5 m depth temperature, salinity, and density fields across the shelf near Cape Hatteras (Figure 9, similar to *Churchill and Berger* [1998, Figure 3]).

[25] In both instances, a clear T, S, and density front is seen extending along the shelf break north of Cape Hatteras and crossing the shelf near the B line. There is cold, fresh, relatively light water north and west of the front (MAB coastal water), and warmer, modestly saline, denser water southward of the front on the shelf (SAB coastal water). This front, termed the "Hatteras Front" by *Churchill and Berger* [1998], is distinct from the Gulf Stream front that

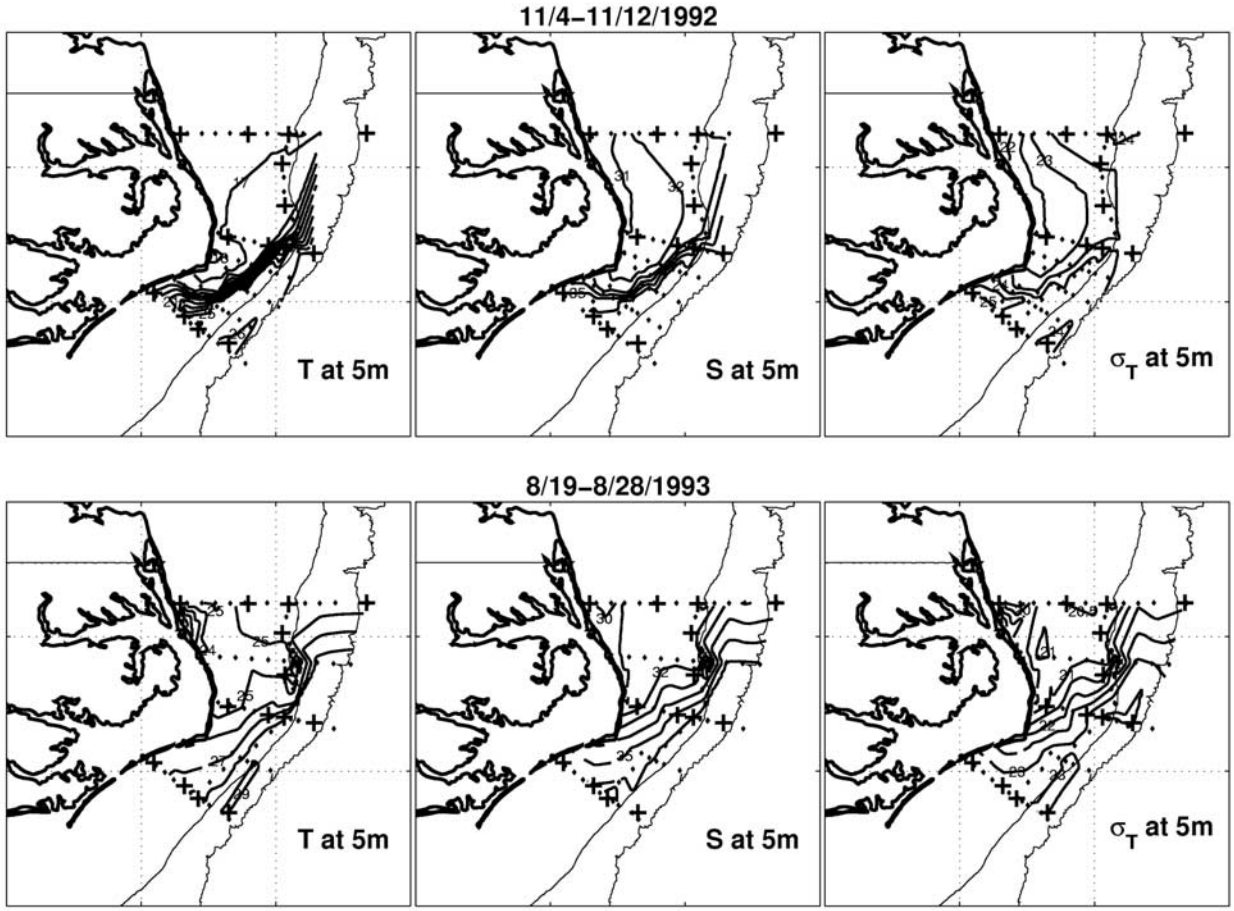

Figure 9. Hydrography at 5 m depth from two cruises: (top) the November 1992 cruise and (bottom) the August 1993 cruise showing (left) temperature (°C), (middle) salinity (psu), and (right) density (σ_t).

runs along the shelf edge south of Cape Hatteras, then separates from the shelf edge and extends seaward to the northeast.

[26] The November 1992 hydrographic cruise fortuitously sampled the nearshore region covered by the extention of the cold fresh MAB water southward past Cape Hatteras (Figure 10). Along-shelf vertical sections of temperature, salinity and density show cold, fresh, relatively light water extending southward past Cape Hatteras, overriding warmer, saltier, unstratified SAB coastal water. Cross-shelf sections of density show that the tongue of light water has separated from the coast by the third south line shown, and does not reach the southernmost cross-shelf line.

[27] The Hatteras Front is visible in many of the non-summer AVHRR SST images collected during the experiment. The daily composites of these images have been pooled and pixel-wise averaged, excluding low-valued pixels that obviously represented cloud cover. Sorting was done into three bins: winter days (October–March) when shoreward currents were observed at $C2_1$, winter days when the currents were northward but not shoreward, and winter days when the currents at $C2_1$ were southward but not shoreward. Each resulting temperature field shows a clear along-shelf temperature gradient, with a front separating cold MAB water from warmer SAB water (Figure 11).

[28] The Front is pushed well southward of Cape Hatteras and Diamond Shoals during days of southward current at $C2_1$. The frontal position is more northward during days of northward current at $C2_1$. The situation during days of shoreward currents at $C2_1$ appears to be something between the northward and southward current situations. This suggests that the shoreward currents may occur as the front advances southward along the coast, along with the wind-forced southward along-shelf flow, or as the front retreats northward. The warm Hatteras Gulf Stream front is also evident, existing right along the shelf edge south of Cape Hatteras, and separating from the shelf edge at and downstream from Cape Hatteras.

6. Cross-Frontal Sea Surface Slope and Density Gradient

[29] If the cross-shelf front separating MAB and SAB shelf waters is dynamically related to the shoreward near-surface currents demonstrated at C2 in section 3, at least two mechanisms accounting for that influence are possible. The first is that the vertical stratification associated with the front

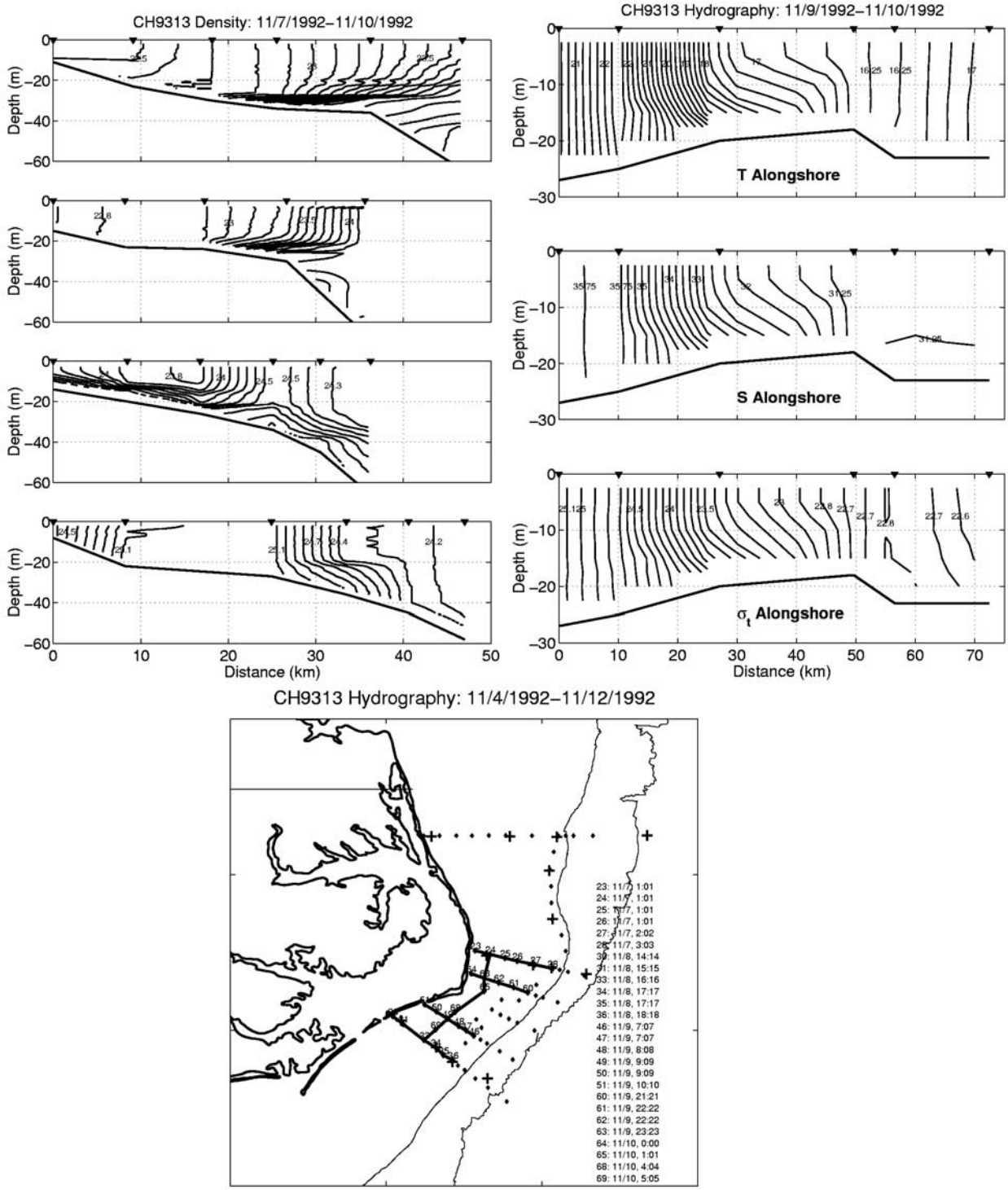

Figure 10. Hydrographic vertical sections from the November 1992 cruise: (left) cross-shelf vertical sections of density for, from top to bottom, a transect coincident with B mooring line; the first transect south of B mooring line; the first transect north of C mooring line; and the transect coincident with C mooring line and (right) alongshore vertical sections (along approximately the 20 m isobath) of (top) temperature, (middle) salinity, and (bottom) density. Station locations are shown at the top of each panel; bottom depths are from cast information. West is to the left in the left panels, south is to the left in the right panels. The bottom panel shows CTD station locations for the November 1992 cruise and sampling dates for the transects shown. The station locations are shown as solid diamonds, and mooring locations are shown as crosses. The 100 and 2000 m isobaths are shown as thin solid lines. Data from station 49 were not included in the alongshore sections.

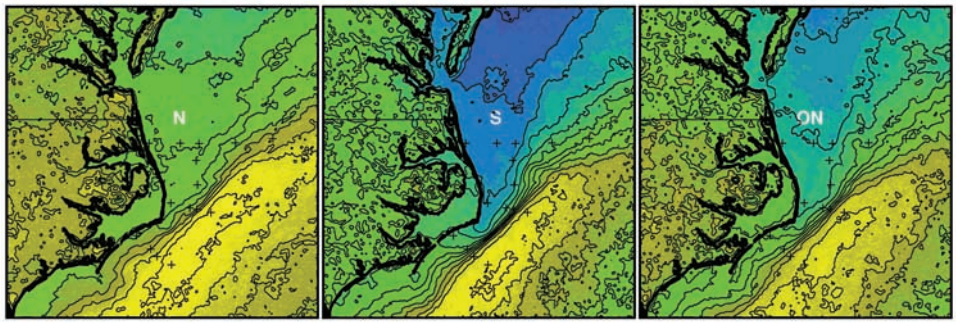

Figure 11. Pixel-wise averaged AVHRR SST with low-value cloud-covered pixels eliminated from averaging technique: (left) winter (October–March) days of northward but not shoreward velocity at $C2_1$, (middle) winter days of southward but not shoreward velocity at $C2_1$, and (right) winter days of shoreward velocity at $C2_1$. Contours have been calculated by smoothing over nine adjacent pixels with a triangular 2-D filter and contouring the smoothed data over the unsmoothed color SST image. Mooring locations are shown as solid diamonds.

sufficiently decouples the top and bottom frictional boundary layers, such that the Ekman drift in the upper layer is enhanced [*Lentz*, 2001]. While upwelling and downwelling cases might show some asymmetry with respect to the effectiveness of this possible mechanism, the sense of the cross-shelf surface flow and vertical shear associated with it should be opposite for upwelling or downwelling favorable winds. However, the shoreward bias in the surface currents occurs under both upwelling or downwelling favorable winds, with northeastward or southwestward along-shelf middepth currents (Figures 12a and 12b). Further, often the shoreward surface currents occur without significant vertical stratification. This suggests that this mechanism is not a good first explanation of how the Hatteras Front might dynamically account for the shoreward flow seen at mooring C2. *Yoder* [1983] also argues against the Ekman drift mechanism as proposed and studied by *Nelson et al.* [1977].

[30] A second possibility is that the cross-frontal sea surface slope and internal horizontal density gradient drive vertically sheared along-front flow. The basic tenet being invoked is that a floating volume of low density water displaces a smaller volume of the underlying denser water column, and so stands up above the surrounding fluid. The resulting sea surface slope at the plume edge could drive an along-front surface velocity through geostrophy. This surface current would be sheared with depth through the thermal wind effect, i.e., the reduction with depth of the surface generated horizontal pressure gradient force by the oppositely directed horizontal pressure gradient force associated with the horizontal density gradient. Using the shallow

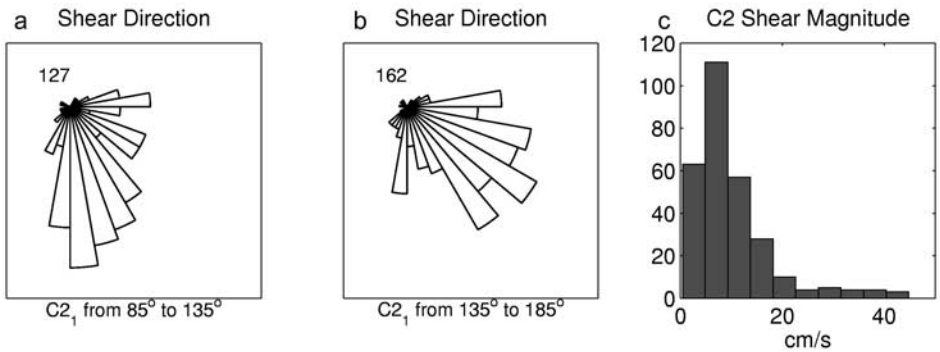

Figure 12. Characterization of vertical shear at mooring C2 during shoreward current events, using 24-HLP data. The direction convention for the shear vectors is such that adding the shear vectors to the 5 m velocity vectors results in the 20 m velocity vectors. (a) Polar histogram of direction of shear on mooring C2 for onshore currents at $C2_1$ directed between 85° and 135° CCW of east, normalized by number of data points; (b) polar histogram of direction of shear on mooring C2 for onshore currents at $C2_1$ directed between 135° and 185° CCW of east, normalized by number of data points; and (c) histogram of magnitudes of shear vectors for onshore currents at $C2_1$ directed between 85 and 185° CCW of east. The numbers printed in Figures 12a and 12b are the number of data points upon which the polar histograms are based. Shear magnitudes are in cm s^{-1} and have not been divided by instrument spacing in the vertical.

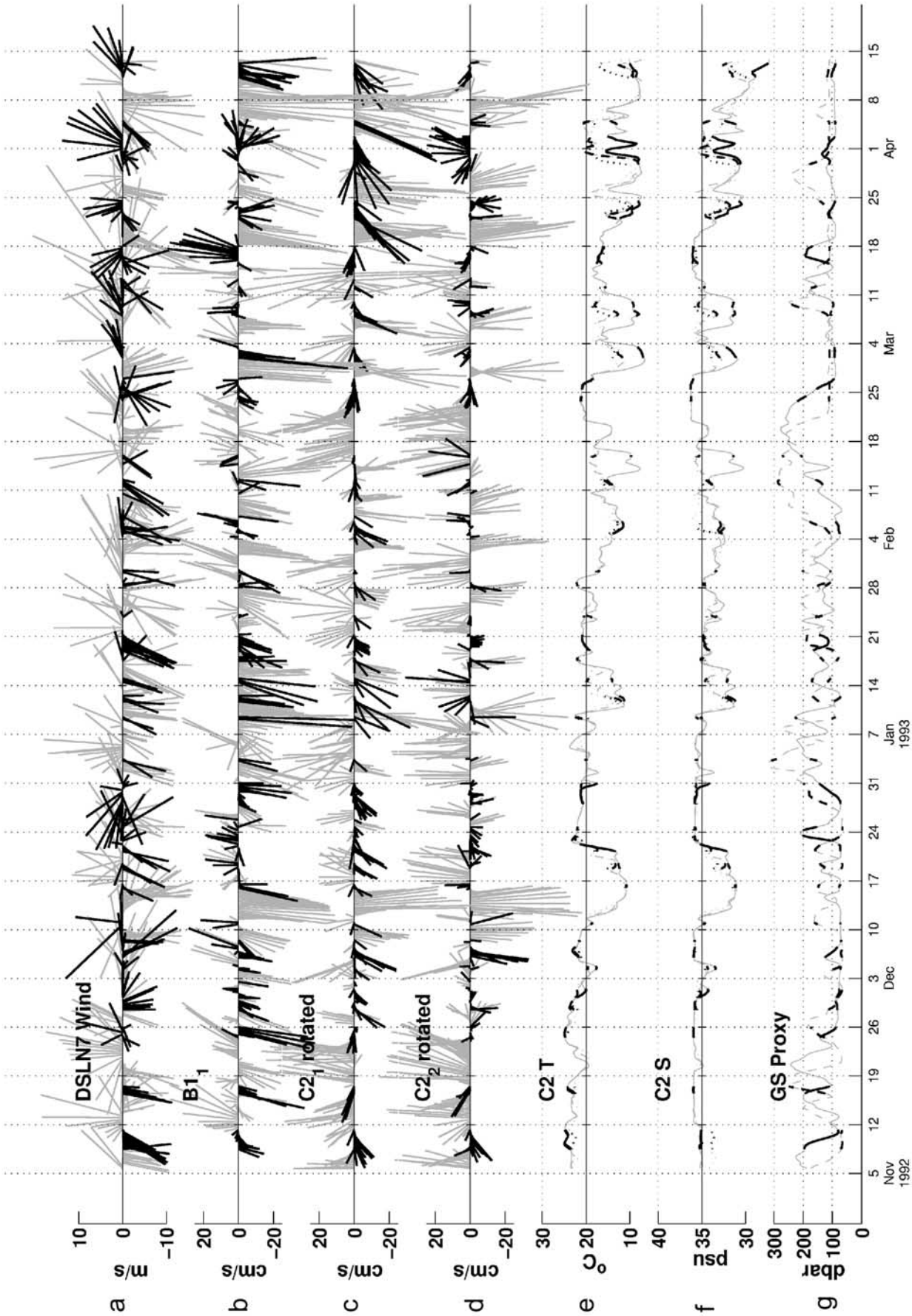
DSLN7 Wind
B1 1
C2 1 rotated
C2 2 rotated
C2 T
C2 S
GS Proxy
a
b
c
d
e
f
g
m/s
cm/s
°C
psu
dbar
5 Nov 1992
12
19
26
3 Dec
10
17
24
31
7 Jan 1993
14
21
28
4 Feb
11
18
25
4 Mar
11
18
25
1 Apr
8
15

water geostrophic equation, the sea surface slope required to support a given geostrophic near-surface velocity is $dH/dy = -uf/g$, where H is the sea surface height, y is the along-shelf direction, positive to the northeast, u is the observed cross-shelf velocity, f is the Coriolis parameter, and g is acceleration due to gravity. Accordingly, a shoreward velocity of $\mathcal{O}$(10 cm/s), as seen here, requires a sea surface slope of approximately 10^{-6} rising to the north, or about 1 cm in 10 km.

[31] To estimate dH/dy from the data, separate estimates of dH and dy are necessary. The sea surface height difference can be calculated by estimating the volume of heavier water displaced by the lighter water using: $\Delta H = h\,(\rho_d - \rho_l)/\rho_l$, where h is the depth of the displaced denser water, ρ_l is the light water density, and ρ_d is the dense water density (*Bowden* [1983] summarizes an equivalent expression in σ_t units). The density records suggest ρ_d and ρ_l both vary by 1–3 σ_t units about a wintertime mean of near 25 σ_t units. For h = 10 m, estimated as the depth to the density interface in the hydrographic sections, and densities in MKS units, this leads to ΔH of $\mathcal{O}$(1 cm).

[32] An estimate of the frontal width across the "nose" of the front (its cross-shelf limb) is possible, by assuming that the velocity measured during frontal passages is all oriented perpendicular to the front. In fact some part of that total might be oriented along the front, and not act to advect it, so that this is an upper bound on the advection speed of the front past the mooring location. A series of frontal passages at C2 were identified as occasions when the magnitude of the temperature change over 6 hours exceeded some threshold. Then the middepth velocities measured at those times were averaged. The length in time of the frontal passages was assessed as the number of sequential data points exhibiting temperature change exceeding the threshold. Both the time and the velocity were robust to threshold values ranging from 0.25 to 1.0°C temperature change over 6 hours. All estimates indicated an average velocity of 0.24 m s^{-1} operating over approximately 1/2 day. This leads to an estimate of about 12 km for the width of the front, just as *Churchill and Berger* [1998] found for the seaward flank of the front. So with an estimate of ΔH of $\mathcal{O}$(1 cm), and y of $\mathcal{O}$(12 km), the sea surface slope required to support the 10 cm/s shoreward velocities is likely satisfied by the nose of the front.

[33] Likewise, the shear associated with the horizontal density gradients can be estimated across an equivalent frontal width as $du/dz = (gd\rho/dy)/(f\rho)$, or approximately 3 cm/s per meter of water column, directed along the density front with lighter water to the left of the shear direction. This can amount to about 45 cm/s difference between the shoreward directed 5 m depth flow and the flow at 20 m depth at C2. Shears of this magnitude are seen in the data, but are more typically less than 20 cm/s difference between the mooring depths during shoreward events (Figure 12c).

7. Examining the Details

[34] A closer examination of the data from the winter of 1992–1993 illustrates the complexity of the task of diagnosing shoreward currents along the C mooring line from the sparse horizontal resolution of this data set. Despite the reasonableness of the along-front current hypothesis, the extent to which along-front shoreward flow can be ascribed on a case-by-case basis is unclear. In the following, several general points will be made quite briefly, with the existence of obvious exceptions acknowledged. Examples and counterexamples of each point are apparent on two figures: (a) 6-hourly data for the complete 1992–1993 winter season (Figure 13) and (b) PVDs from daily data and 6-hourly time series for a 7-week period at the end of this same winter (Figure 14).

[35] The reader is invited to scrutinize these figures carefully to assess the degree to which the following points generally hold. The event-like nature of the shoreward flow will become apparent, illustrating the inadequacy of conventional time series analysis tools for the evaluation of the suggested correlations.

1. The seasonal correlations that were evident in the 2-year time series of 48-HLP data (Figure 5) appear to also hold through the winter season itself on an event-by-event basis, over timescales of several days to a week: strong correlations exist between the along-shelf component of the wind and along-shelf currents at B1 and C2, and between the predominantly along-shelf currents at B1 and C2. There is also a clear correlation between instances of prolonged southward along-shelf currents at B1 and the advection of a temperature and salinity front across the C2 mooring location.

2. Shoreward currents are primarily associated with southwestward wind, particularly the ends of episodes of several days duration. Predominantly southward flow at B1 is also associated with these periods of shoreward surface currents at C2. Shoreward currents at C2 are often accompanied by shoreward currents at C1.

3. However, the shoreward currents along the C line occur under both upwelling and downwelling favorable wind conditions. The direction of the shoreward currents is

Figure 13. (opposite) Selected time series for winter, 1992–1993: (a) DSLN7 12-HLP wind, (b) $B1_1$ 24-HLP currents, (c) $C2_1$ 24-HLP rotated currents, (d) $C2_2$ 24-HLP rotated currents, (e) C2 24-HLP temperature (all depths), (f) C2 24-HLP salinity (corrected, all depths), and (g) Gulf Stream relative distance offshore. C2 currents were rotated 64° CCW so that the positive y axis corresponds with along-shelf to the northeast. The wind and B1 vectors are oriented so that north is aligned with the positive y axis. Solid vectors and lines represent data collected while the (unrotated) currents at $C2_1$ were oriented between 85° and 185° CCW of eastward, while the shaded vectors represent all other data. In Figures 13e and 13f, solid lines represent data from 5 m depth, dashed lines represent data from 20 m depth, and dotted lines represent data from 30 m depth. In Figure 13g, The solid line represents Gulf Stream distance offshore along the B line, and the dashed line represents Gulf Stream distance offshore along the C line. Larger values in Figure 13g represent more shoreward Gulf Stream positions.

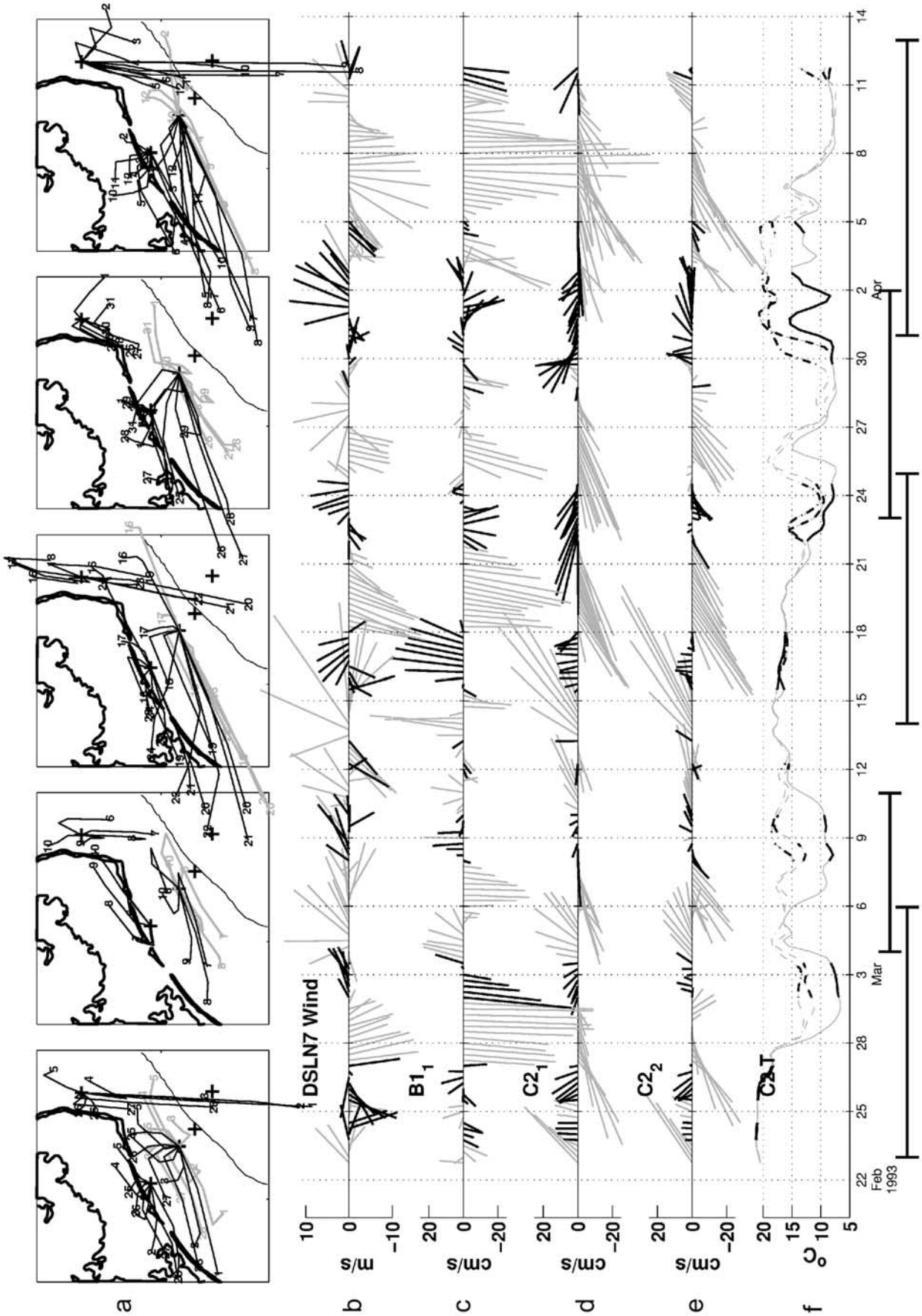
a
b
c
d
e
f
DSLN7 Wind
B1$_1$
C2$_1$
C2$_2$
C2$_T$
m/s
cm/s
°C
22
Feb
1993
Mar
Apr

seen to sweep from northeast to southwest and back again over several 4–6 day periods. (This is particularly evident in the PVD plots.) These sweeps occur primarily in a shoreward direction, regardless of the CW or CCW sense of turning of the wind.

4. Large vertical shear at mooring C2 is evident during or immediately preceeding many shoreward flow events. This shear is particularly evident in the PVD plots, but also in the time series plots. The magnitude of this shear can amount to several tens of degrees difference between current direction at $C2_1$, and $C2_2$. This is true whether the vertical mean current is more southwestward or northeastward. In either case, the shear vector is such that surface currents are more shoreward than the predominantly along-shelf oriented middepth currents.

8. Discussion

[36] Shoreward transport mechanisms south of Cape Hatteras must exist in order to account for the success of many offshore spawning, estuarine-dependant fauna. The references listed in section 1 used indirect methods to demonstrate that (especially surface) shoreward flow would be consistent with several different mechanisms. Here, for the first time, that shoreward flow in Raleigh Bay has been measured in situ and documented. The shoreward velocities are sufficiently energetic and persistent to transport passive particles across the shelf. The events are frequent enough to assure many opportunities for such shoreward transport to occur through the winter season, not only at the C line, but wherever the cross-shelf front regularly migrates in winter. Shoreward flow along the Hatteras Front should represent a reliable conduit for shoreward transport on an annual basis, as the front separating climatologically different shelf water masses is advected along-shelf by wind and Gulf Stream forcing whose characteristics do not change significantly from year to year. The observation of the shoreward currents in each of the three consecutive winters sampled by this experiment suggests their poten-tial recurrence.

[37] Previous studies of the shelf south of Cape Hatteras give some indication of the along-shelf distance that the Hatteras Front may travel through a given year. The shoreward currents and large temperature and salinity changes observed in summer at mooring B1 suggest that the cross-shelf part of the Hatteras Front resides northward of Cape Hatteras in the summer, under the prevailing northwestward winds. *Stegmann and Yoder* [1996] found that the nose of the Hatteras Front often extended south past Cape Hatteras, and occasionally intruded past Cape Lookout into Onslow Bay. Their analysis of 5 years of AVHRR SST images indicated that the nose of the Hatteras Front progressed past Cape Lookout at least two and up to eight times every year. *Pietrafesa et al.* [1994] estimated that MAB shelf water reaches as far south as Frying Pan Shoals, off Cape Fear at the southern end of Onslow Bay, approximately 10% of the time over a 7 year data record. If the average frontal advection speed calculated here of ~24 cm/s applied to advection alongshore throughout Raleigh Bay, the front would be able to traverse the ~115 km length of the bay in less than 6 days. Assuming the southward progression of the front is driven by along-shelf wind, several occasions of frontal progression past Cape Lookout ought to be expected every year, since several occasions of prolonged strong southward along-shelf winds occur yearly. The predominance of southward over northward winds in winter in this location might result in some rectification of the frontal location southward over the winter. There is some suggestion of this in the satellite imagery (not shown).

[38] The Gulf Stream may play some role in the shoreward flow events, with shoreward and southward flow at C2 both associated with a more seaward Gulf Stream position. The Gulf Stream may modulate how the shelf water responds to southward along-shelf winds, and may play some role in the northward advection of the Hatteras Front following its southward excursions. *Stegmann and Yoder* [1996] suggest that Gulf Stream filaments may interact with the extension of the Hatteras Front into Raleigh Bay, altering the width or along-shelf structure of the cold water tongue. This analysis does not rule out direct filament-related shoreward advection south of Cape Hatteras, the favored hypothesis of *Stegmann and Yoder* [1996]. But the Gulf Stream effect on the process described herein is likely indirect.

[39] **Acknowledgments.** Support for this study came from the Center for Coastal Physical Oceanography, Old Dominion University, Norfolk, Va. The data were collected for the Minerals Management Service OCS Study MMS 94-0047. Comments from Jack Blanton and John Bane on an early draft were quite helpful.

References

Atkinson, L. P., Modes of Gulf Stream intrusion into the South Atlantic Bight shelf waters, *Geophys. Res. Lett.*, *4*, 583–586, 1977.

Berger, T. J., P. Hamilton, R. J. Wayland, J. O. Blanton, W. C. Boicourt, J. H. Churchill, and D. R. Watts, A physical oceanographic field program offshore North Carolina, *Tech. Rep. OCS Study MMS 94-0047*, U. S. Dep. of the Inter., Miner. Manage. Serv., New Orleans, La., 1995.

Bowden, K. F., *Physical Oceanography of Coastal Waters*, 302 pp., Halstead, New York, 1983.

Bumpus, D. F., A description of the circulation on the continental shelf of the east coast of the United States, *Prog. Oceanogr.*, *6*, 111–157, 1973.

Chapman, D. C., and R. C. Beardsley, On the origin of shelf water in the Middle Atlantic Bight, *J. Phys. Oceanogr.*, *19*, 384–391, 1989.

Checkley, D. M., S. Raman, G. L. Maillet, and K. M. Mason, Winter storm effects on the spawning and larval drift of a pelagic fish, *Nature*, *335*, 346–348, 1988.

Figure 14. (opposite) Progressive vector diagrams and time series for February 23, 1993, through April 11, 1993. (a) Three-day PVDs from 48-HLP data, with ending dates plotted at PVD endpoints. The solid lines represent 5 m data; the shaded lines represent data from the next level down. Time series panels: (b) DSLN7 12-HLP wind,(d) $B1_1$ 24-HLP currents,(d) $C2_1$ 24-HLP unrotated currents, (e) $C2_2$ 24-HLP unrotated currents, and (f) C2 24-HLP temperature (all depths). In the stick plots, north is aligned with the positive y axis. Solid vectors and lines represent data collected while the currents at $C2_1$ were oriented between 85° and 185° CCW of eastward, while the shaded vectors represent all other data. In Figure 14f solid lines represent data from 5 m depth, dashed lines represent data from 20 m depth, and dotted lines represent data from 30 m depth.

Churchill, J. H., and T. J. Berger, Transport of Middle Atlantic Bight shelf water to the Gulf Stream near Cape Hatteras, *J. Geophys. Res.*, *103*, 30,605–30,622, 1998.

Hogg, N. G., Mooring motion corrections revisited, *J. Atmos. Oceanic Technol.*, *8*, 289–295, 1991.

Lentz, S. J., The influence of stratification on the wind-driven cross-shelf circulation over the North Carolina shelf, *J. Phys. Oceanogr.*, *31*, 2749–2760, 2001.

Madsen, O. S., A realistic model of the wind-induced Ekman boundary layer, *J. Phys. Oceanogr.*, *7*, 248–255, 1977.

Nelson, W. R., M. C. Ingham, and W. E. Schaaf, Larval transport and year-class strength of Atlantic menhaden, *Brevoortia tyrannus*, *Fish. Bull. U. S.*, *75*, 23–41, 1977.

Pietrafesa, L. J., J. M. Morrison, M. P. McCann, J. Churchill, E. Bohm, and R. W. Houghton, Water mass linkages between the Middle and South Atlantic Bights, *Deep Sea Res., Part II*, *41*, 365–389, 1994.

Quinlan, J. A., B. Blanton, T. Miller, and F. Werner, From spawning grounds to the estuary: Using linked individual based and hydrodynamic models to interpret patterns and processes in the oceanic phase of Atlantic menhaden Brevoortia tyrannus life history, *Fish. Oceanogr.*, *8*, 224–246, suppl. 2, 1999.

Savidge, D. K., and J. M. Bane, Wind and Gulf Stream influences on along-shelf transport and off-shelf export at Cape Hatteras, North Carolina, *J. Geophys. Res.*, *106*, 11,505–11,527, 2001.

Shanks, A. L., Further support for the hypothesis that internal waves can cause shoreward transport of larval invertebrates and fish, *Fish. Bull. U. S.*, *86*, 703–714, 1988.

Stefansson, L., P. Atkinson, and D. F. Bumpus, Hydrographic properties and circulation of the North Carolina shelf and slope waters, *Deep Shelf Res.*, *18*, 383–420, 1971.

Stegmann, P. M., and J. A. Yoder, Variability of sea-surface temperature in the South Atlantic Bight as observed from satellite: Implications for off-shore spawning fish, *Cont. Shelf Res.*, *16*, 843–861, 1996.

Yoder, J. A., Statistical analysis of the distribution of fish eggs and larvae on the southeastern U. S. continental shelf with comments on oceanographic processes that may affect larval survival, *Estuarine Coastal Shelf Sci.*, *17*, 637–650, 1983.

D. K. Savidge, Center for Coastal Physical Oceanography, Department of Ocean, Earth and Atmospheric Sciences, Old Dominion University, Norfolk, VA 23529, USA. (savidge@ccpo.odu.edu)